J|A|C|S
ARTICLES
Published on Web 04/07/2006

A Strategy for the Analysis of Chiral Polyoxotungstates by Multinuclear (^{31}P, ^{183}W) NMR Spectroscopy Applied to the Assignment of the ^{183}W NMR Spectra of α_1-$[P_2W_{17}O_{61}]^{10-}$ and α_1-$[YbP_2W_{17}O_{61}]^{7-}$

Géraldine Lenoble, Bernold Hasenknopf, and René Thouvenot*

Contribution from the Université Pierre et Marie Curie - Paris 6, Institut de Chimie Moléculaire FR 2769, Laboratoire de Chimie Inorganique et Matériaux Moléculaires (UMR CNRS 7071), Case Courrier 42, 4 place Jussieu, 75252 Paris Cedex 05, France

Received November 21, 2005; E-mail: rth@ccr.jussieu.fr

Abstract: This paper describes the complete assignment of the ^{183}W NMR spectra of the chiral polyoxometalates α_1-$[P_2W_{17}O_{61}]^{10-}$ and α_1-$[YbP_2W_{17}O_{61}]^{7-}$ in aqueous solution. These spectra display each 17 lines of equal intensity with a relatively narrow chemical shift distribution. The identification of signals is based on selective ^{31}P−^{183}W decoupling and recognition of particular sets of coupling constants for tungsten atoms around the lacunary site. Further assignment is obtained by ^{183}W 2D-COSY NMR experiments. We demonstrate herewith a new way for the unambiguous assignment of ^{183}W NMR spectra of polyoxotungstates without any symmetry elements or tungsten atoms in special positions. This way relies on the correlation of the magnitude of $^2J_{W-W}$ coupling constants with the geometry of oxo-bridges in polyoxotungstates. These results open the way to monitor interaction sites of chiral polyoxotungstates with organic ligands.

Introduction

Polyoxometalates (POMs) are polymetallic cluster compounds presenting a very large diversity of structures. The use of ^{183}W NMR for the characterization of polyoxotungstates is more and more common, despite the relative poor receptivity of the ^{183}W nucleus, which is around 5 orders of magnitude lower than that of ^{1}H.[1−4] ^{183}W is the fifth less receptive spin $^1/_2$ nucleus. For this reason, spectra with a satisfactory signal-to-noise ratio can only be obtained in nonprohibitive times from fairly concentrated solutions ($\gg$0.1 M) even on modern high-field spectrometers.[5] The number and intensities of resonance lines provide direct information on the sets of nonequivalent tungsten atoms and can be related to a given structure. Usually symmetry considerations, sometimes combined with observations of particular chemical shifts, are employed to confirm or reject a structural proposal.[6,7] However, the complete assignment of all signals in a spectrum to W atoms of a polyoxotungstate is not yet routinely done. Such an assignment not only reveals the structural characteristics of the compound but also can give insight into electronic features across the tungsten shell. Moreover, reactions can be followed with respect to the site where they are happening. Finally, a deeper understanding of ^{183}W NMR spectra will facilitate the elucidation of new structures where other structural evidence is unavailable.

It has been recognized that ^{183}W chemical shifts are extremely sensitive to tiny structural changes.[1,2,5] That means that each set of equivalent tungsten atoms in an unsymmetrical polyoxotungstate is characterized by a distinct resonance line. However, for a given polyoxotungstate, it is nearly impossible at the present time to predict the positions of the different lines, even by computational methods.[8,9] Conversely, it remains impossible to assign signals from the ^{183}W chemical shifts, except for individual tungsten atoms in a very special environment.[10] The careful analysis of signal intensity and peak height allows the assignment of ^{183}W spectra of some diamagnetic polyoxotungstates.[11]

As a rule, the assignment of the ^{183}W resonances to the structurally unequivalent W atoms of the polyoxometalate framework may be done using J_{W-W} coupling constants, which allow us to establish the W−W connectivity.[6,7] A typical ^{183}W peak in diamagnetic species is of narrow line width ($\leq$ 1 Hz).[5] Satellite peaks of 7% intensity of the signal reveal geminal W−W coupling, provided sufficient signal-to-noise ratio, and no overlap with the base of the central resonance. However, in

(1) Chen, Y.-G.; Gong, J.; Qu, L.-Y. *Coord. Chem. Rev.* **2004**, *248*, 245−260.
(2) Kazansky, L. P.; McGarvey, B. R. *Coord. Chem. Rev.* **1999**, *188*, 157−210.
(3) Minelli, M.; Enemark, J. H.; Brownlee, R. T. C.; O'Connor, M. J.; Wedd, A. G. *Coord. Chem. Rev.* **1985**, *68*, 169−278.
(4) *NMR and the periodic table*; Harris, R. K., Mann, B. E., Eds.; Academic Press: London, U.K., 1978.
(5) Acerete, R.; Hammer, C. F.; Baker, L. C. W. *J. Am. Chem. Soc.* **1979**, *101*, 267−269.
(6) Domaille, P. J.; Knoth, W. H. *Inorg. Chem.* **1983**, *22*, 818−822.
(7) Lefebvre, J.; Chauveau, F.; Doppelt, P.; Brevard, C. *J. Am. Chem. Soc.* **1981**, *103*, 4589−4591.
(8) Bagno, A.; Bonchio, M.; Sartorel, A.; Scorrano, G. *ChemPhysChem* **2003**, *4*, 517−519.
(9) Kazansky, L. P.; Chaquin, P.; Fournier, M.; Herve, G. *Polyhedron* **1998**, *17*, 4353−4364.
(10) Sadakane, M.; Dickman, M. H.; Pope, M. T. *Inorg. Chem.* **2001**, *40*, 2715−2719.
(11) Sveshnikov, N. N.; Pope, M. T. *Inorg. Chem.* **2000**, *39*, 591−594.

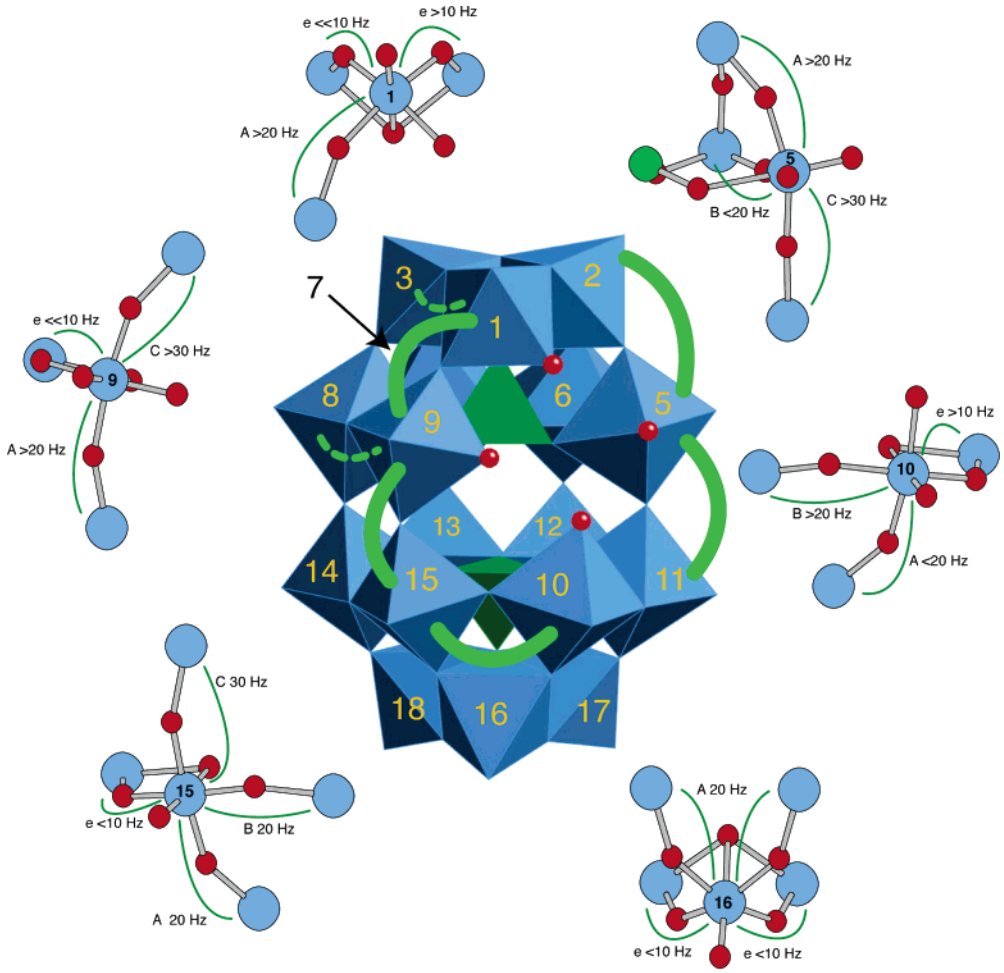

Figure 1. α_1-$[P_2W_{17}O_{61}]^{10-}$ in polyhedral representation with numbering of the tungsten atoms. The green lines indicate the anticipated exceptionally strong (thick line) or weak (dotted line) $^2J_{W-W}$ coupling of the tungsten atoms around the vacant site. The ball-and-stick representation of these tungsten atoms shows the geometry of the oxo bridges, together with the expected magnitude of the $^2J_{W-W}$ coupling constants. e = edge, A = cap−belt corner, B = intraunit belt−belt corner, C = interunit belt−belt corner coupling.

polyoxometalates, all tungsten atoms have three to four coupling partners, and in large unsymmetrical structures, it is nearly impossible to measure all coupling constants, many of them having very close values. Heteronuclear coupling often complicates the situation even further. For instance in phosphotungstates, each resonance, central line and its tungsten satellites, becomes a doublet.

Correlation spectroscopy, such as 2D-COSY and 2D-INADEQUATE, has proven to be helpful for establishing the connectivity, in particular when $^2J_{W-W}$ constants are similar.[6,12] However, in every case a suitable starting point is required. This may be a tungsten in a special easily recognized position: for instance location on a symmetry element, leading to a less intense signal,[13] or vicinity of a magnetically active heteronucleus, resulting in heteronuclear coupling.[14,15] To the best of our knowledge, no structural assignment of a ^{183}W NMR spectrum without such an entrance has been reported.

We are interested in particular in the intermolecular interactions between chiral polyoxometalates, here α_1-$[P_2W_{17}O_{61}]^{10-}$ and α_1-$[YbP_2W_{17}O_{61}]^{7-}$, and organic molecules. ^{183}W NMR is the technique of choice because the variations in the spectra on complex formation reflect the changes of the chemical environment at each tungsten site. To obtain a complete map of the intermolecular interactions, all the signals must first be assigned to the individual W atoms in both POMs. The structure of α_1-$[P_2W_{17}O_{61}]^{10-}$ (shortly α_1-P_2W_{17}) derives from the Dawson structure of α-$[P_2W_{18}O_{62}]^{6-}$ by eliminating formally one $\{WO\}^{4+}$ unit from a belt (Figure 1). α_1-$[P_2W_{17}O_{61}]^{10-}$ (C_1 symmetry) is thermodynamically unstable, and by migration of the vacancy from the belt to the cap, it transforms slowly in solution into its more symmetrical isomer α_2-$[P_2W_{17}O_{61}]^{10-}$ (C_s symmetry). The lacuna serves as a ligand for lanthanides such as Yb^{3+} in α_1-$[YbP_2W_{17}O_{61}]^{7-}$ (shortly α_1-YbP_2W_{17}).[10,16−19]

For α_1-$[P_2W_{17}O_{61}]^{10-}$ and α_1-$[YbP_2W_{17}O_{61}]^{7-}$, because of the lack of any symmetry element, the 17 W atoms are

(12) Brevard, C.; Schimpf, R.; Tourne, G.; Tourne, C. M. *J. Am. Chem. Soc.* **1983**, *105*, 7059−7063.
(13) Cadot, E.; Thouvenot, R.; Tézé, A.; Hervé, G. *Inorg. Chem.* **1992**, *31*, 4128−4133.
(14) Canny, J.; Thouvenot, R.; Tézé, A.; Hervé, G.; Leparulo-Loftus, M.; Pope, M. T. *Inorg. Chem.* **1991**, *30*, 976−981.
(15) Thouvenot, R.; Tézé, A.; Contant, R.; Hervé, G. *Inorg. Chem.* **1988**, *27*, 524−529.
(16) Zhang, C.; Howell, R. C.; Luo, Q.-H.; Fieselmann, H. L.; Todaro, L. J.; Francesconi, L. C. *Inorg. Chem.* **2005**, *44*, 3569−3578.
(17) Luo, Q.-H.; Howell, R. C.; Dankova, M.; Bartis, J.; Williams, C. W.; Horrocks, W. D., Jr.; Young, V. G.; Rheingold, A. L.; Francesconi, L. C.; Antonio, M. R. *Inorg. Chem.* **2001**, *40*, 1894−1901.
(18) Bartis, J.; Dankova, M.; Lessmann, J. J.; Luo, Q.-H.; Horrocks, W. D., Jr.; Francesconi, L. C. *Inorg. Chem.* **1999**, *38*, 1042−1053.
(19) Ciabrini, J.-P.; Contant, R. *J. Chem. Res., Synop.* **1993**, 391.

unequivalent and the ^{183}W NMR spectra exhibit 17 lines of same intensity. The spectra of α_1-$[P_2W_{17}O_{61}]^{10-}$ and several of its lanthanide complexes have been reported as such without assignment, as there is no starting point as those described above.[10,16,20−22]

We demonstrate in the following that it is nevertheless possible to make a complete and unambiguous assignment of the spectra, based on (i) the 2D-COSY correlations, (ii) the homonuclear coupling constants values, and (iii) the results of ^{31}P-selective decoupling experiments.

Results and Discussion

General Observations. A. ^{31}P NMR of α_1-$[P_2W_{17}O_{61}]^{10-}$ and α_1-$[YbP_2W_{17}O_{61}]^{7-}$. The ^{31}P NMR spectra of α_1-$[P_2W_{17}O_{61}]^{10-}$ and α_1-$[YbP_2W_{17}O_{61}]^{7-}$ have been reported.[18,22] The chemical shifts depend on the composition of the solution (concentration, counterions) and the temperature. Under the conditions of the ^{183}W 2D spectra discussed below, $\delta(^{31}P)$ for the PW_8O_{33} unit (shortly PW_8) in α_1-$[P_2W_{17}O_{61}]^{10-}$ is −8.57 ppm and for the PW_9O_{34} unit (shortly PW_9) is −12.88 ppm. The presence of the paramagnetic Yb^{3+} (electron configuration $4f^{13}$) in α_1-$[YbP_2W_{17}O_{61}]^{7-}$ induces some line broadening and a large paramagnetic shift to $\delta(^{31}P) = 37.4$ ppm for PW_8Yb and 3.8 ppm for PW_9.

B. Homonuclear Tungsten−Tungsten Coupling. Some general trends for tungsten−tungsten couplings as a function of the geometrical features of the W−O−W bridge, i.e., W−O−W angle and W−O bond lengths, have been deduced from a range of ^{183}W NMR experimental analyses of polyoxotungstates. Actually, as first noted by Brevard et al. on Keggin anions and further extended to Dawson anions by one of us,[7,23] for unsubstituted saturated polyoxotungstates, essentially three types of homonuclear $^2J_{W-W}$ coupling constants are observed, depending on the angle α of the W−O−W bridge. Edge couplings (between tungsten atoms sharing two oxo ligands; α ca. 120°) are generally smaller than 10 Hz, while the corner couplings (between tungsten atoms sharing one oxo ligand; α ca. 150° in Keggin and in Dawson POMs; α ca. 160° for the XW_9-XW_9 (X = As, P) interunit junction in Dawson POMs) are in the range of 20 and 30 Hz, respectively. These couplings are modified in lacunary species due to the trans influence of the terminal oxo ligands. As the W−O bond trans to an O_{term} is longer than a W−O bond trans to an O_{bridge}, the W−O bonds trans to the oxygens forming the lacuna are elongated. The couplings through these W−O−W bridges are therefore weakened. At the same time, an enhancement of the coupling to the other two W neighbors is observed.[24,25] Thus, a W atom bordering the lacuna has one coupling smaller and two couplings larger than usual. Recent DFT calculations have confirmed that the $^2J_{W-W}$ coupling constants depend on the angle α and the W−O bond length and have shown that the electronic structure of the surroundings farther than one bond away does not affect these couplings significantly.[26] The relationship between structure and coupling constants is therefore well established, from both experiment and theory. Figure 1 resumes these effects and shows the expected range of coupling constants for the different types of W atoms. The green lines highlight the sites where a particularly strong (thick line) or a particularly weak (dotted line) coupling is expected. Table 1 compiles the connectivity of all W atoms in α_1-$[P_2W_{17}O_{61}]^{10-}$ (and α_1-$[YbP_2W_{17}O_{61}]^{7-}$).

C. Heteronuclear ^{183}W−^{31}P Coupling. For P-centered POMs, because of heteronuclear $^2J_{W-P}$ coupling, each ^{183}W line is expected to appear as a doublet. Indeed, the pioneering works of Acerete et al. on very low field ^{183}W spectra report "baseline resolved doublets" for $[PW_{12}O_{40}]^{3-}$ and other tungstophosphates.[5] However, for the subsequent higher-field ^{183}W NMR investigations of P-centered POMs, the splitting due to ^{31}P−^{183}W coupling is less easily observable and sometimes undetected even under resolution enhancement. This effect is assigned to the increase of the ^{183}W relaxation rate with increasing magnetic field, (vide infra) resulting in increasing line width, exceeding the $^2J_{W-P}$ couplings. In the present work, the $^2J_{W-P}$ splitting is generally observed at 12.5 MHz (AC300), while at higher field (20.8 MHz, DRX500) the lines become broader and only some lines are hardly split.

In principle, cap and belt W atoms may be recognized by their $^2J_{W-P}$ couplings, as belt couplings are generally larger (ca. 2 Hz) than cap couplings (ca 1 Hz),[27] but this rule appears more questionable in lacunary species (see discussion below). Broad-band ^{31}P decoupling leads all doublets to coalesce into singlets, whereas selective ^{31}P decoupling allows to discriminate those W belonging to the PW_9 unit from those of the PW_8 unit.[28]

NMR Spectra of α_1-$[P_2W_{17}O_{61}]^{10-}$. A. Partial Assignment to Each PW_9 or PW_8 Subunit of α_1-$[P_2W_{17}O_{61}]^{10-}$. The lower part of Figure 2 presents the 12.5 MHz ^{183}W spectrum of α_1-$[P_2W_{17}O_{61}]^{10-}$ obtained without ^{31}P decoupling; all signals appear as more of less resolved doublets except the **e** signal which remains a single resonance after resolution enhancement. For this **e** signal, $^2J_{W-P}$ coupling is however ascertained by the low-intensity antiphase doublet resulting from ^{31}P−^{183}W INEPT transfer (Figure 2, upper trace). The $^2J_{W-P}$ coupling constants are compiled in Table 2. Under broad-band ^{31}P decoupling, all doublets coalesce into narrow singlets, whereas the **e** resonance hardly sharpens (Figure 3, lower trace). On selective ^{31}P decoupling from the more shielded ^{31}P nucleus (−12.88 ppm), nine ^{183}W signals **d**, **h**, **i**, **l**, **m**, **n**, **o**, **p**, and **q** no longer appear as doublets (Figure 3, top trace, blue signals). These peaks therefore arise from the PW_9 subunit, and consequently the remaining eight signals **a**, **b**, **c**, **e**, **f**, **g**, **j**, and **k** arise from W atoms of the PW_8 subunit. Actually by selective ^{31}P decoupling from the deshielded ^{31}P nucleus (−8.57 ppm), the seven doublets **a**, **b**, **c**, **f**, **g**, **j**, and **k** become singlets (Figure 3 middle trace, red signals). Even if signal **e** is nearly unaffected, whatever the ^{31}P decoupling conditions, its assignment by deduction to the PW_8 subunit is nevertheless unequivocal.

B. Analysis of the 2D-COSY Spectrum of α_1-P_2W_{17}. The 2D-COSY spectrum of α_1-$[P_2W_{17}O_{61}]^{10-}$, registered at 283 K to slow the $\alpha_1-\alpha_2$ isomerization, is presented in Figure 4. According to the connectivity matrix, 64 cross-peaks are

(20) Bartis, J.; Sukal, S.; Dankova, M.; Kraft, E.; Kronzon, R.; Blumenstein, M.; Francesconi, L. C. *J. Chem. Soc., Dalton Trans.* **1997**, 1937−1944.
(21) Bartis, J.; Dankova, M.; Blumenstein, M.; Francesconi, L. C. *J. Alloys Compd.* **1997**, *249*, 56−68.
(22) Bartis, J.; Kunina, Y.; Blumenstein, M.; Francesconi, L. C. *Inorg. Chem.* **1996**, *35*, 1497−1501.
(23) Contant, R.; Thouvenot, R. *Inorg. Chim. Acta* **1993**, *212*, 41−50.
(24) Canny, J.; Tézé, A.; Thouvenot, R.; Hervé, G. *Inorg. Chem.* **1986**, *25*, 2114−2119.
(25) Mayer, C. R.; Thouvenot, R. *J. Chem. Soc., Dalton Trans.* **1998**, 7−13.
(26) Bagno, A.; Bonchio, M. *Angew. Chem., Int. Ed.* **2005**, *44*, 2023−2026.
(27) Contant, R.; Abbessi, M.; Thouvenot, R.; Hervé, G. *Inorg. Chem.* **2004**, *43*, 3597−3604.
(28) Finke, R. G.; Droege, M. W.; Domaille, P. J. *Inorg. Chem.* **1987**, *26*, 3886−3896.

Table 1. Theoretical Connectivity Matrix for α_1-$[P_2W_{17}O_{61}]^{10-}$ and α_1-$[YbP_2W_{17}O_{61}]^{7-}$ [a]

W	1	2	3	5	6	7	8	9	10	11	12	13	14	15	16	17	18	Particular Couplings
1	δ	e/w	e/vw					A/S										1 S, 1w, 1 vw
2	e/w	δ	e/w	A/S	A													
3	e/vw	e/w	δ			A	A											
5		A/S		δ	B/w					C/S								2 S, 1 m
6		A		B/w	δ	e/w					C							
7			A		e/w	δ	B					C						
8			A			B	δ	e/vw					C					
9	A/S						e/vw	δ						C/S				2 S, 1 vw
10									δ	e/s				B/S	A/w			1 VS, 2 m
11				C/S					e/s	δ	B					A		
12					C					B	δ	e				A		
13						C					e	δ	B				A	
14							C					B	δ	e/w			A	
15								C/S	B/S				e/w	δ	A			2VS, 1 S, 1 w
16									A/w					A	δ	e	e	
17										A	A				e	δ	e	
18												A	A		e	e	δ	

[a] The empirical order of coupling constants is e (edge) < A (cap−belt corner) ≈ B (intraunit belt−belt corner) < C (interunit belt−belt corner). Expected modifications due to the lacuna are noted: vw = very weaker, w = weaker, S = stronger than usual. Numbering of W according to Figure 1; bold numbers indicate W bordering the lacuna.

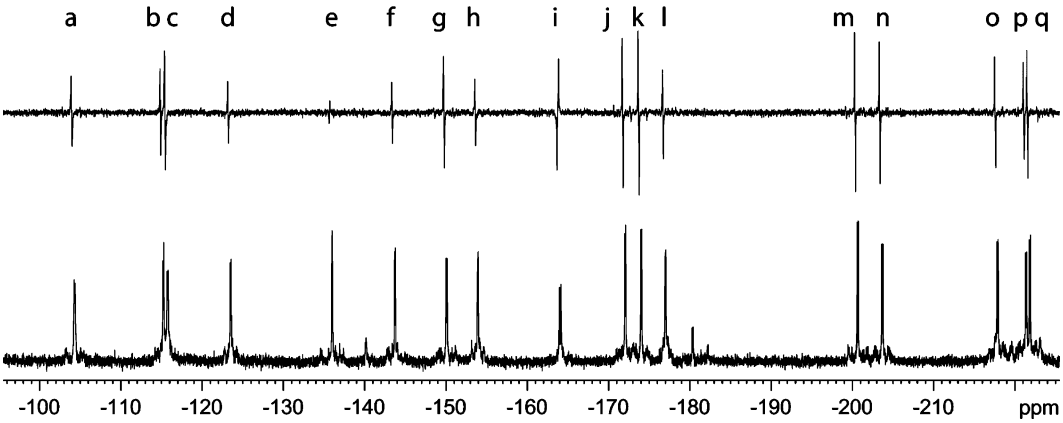

Figure 2. 12.5 MHz ^{183}W NMR spectrum of α_1-$[P_2W_{17}O_{61}]^{10-}$ (2.5 g/mL) (bottom trace) and INEPT spectrum (top trace). Denomination of the signals as given throughout the text is from left (peak **a**) to right (peak **q**).

Table 2. $^2J_{W-P}$ Coupling Constants (Hz)

$^2J_{W-P}$ (Hz)	a	b	c	d	e	f	g	h	i	j	k	l	m	n	o	p	q
α_1-$[P_2W_{17}O_{61}]^{10-}$	1.4	1.2	1.2	1.0	<0.5	0.9	1.5	1.1	2.4	1.4	1.4	1.2	1.6	1.5	1.6	1.8	1.6
α_1-$[YbP_2W_{17}O_{61}]^{7-}$		1.9			0.8			1.0				0.5	1.5	1.5	1.6	1.3	1.7

expected. Only 56 are unequivocally identified, because those near the diagonal are questionable, and correlations through small $^2J_{W-W}$ couplings likely lead to low intensity well under the noise level.

The 2D spectrum of Figure 4 is translated into an experimental connectivity matrix (Table 3) giving the chemical shift values and the coupling constants. Under the relatively high resolution of the 2D spectrum (1 Hz/pt), the $^2J_{W-W}$ values larger than 10 Hz are directly accessible by row analysis (Figure 5).

We consider first the five cross-peaks resulting from the largest couplings, i.e., >27 Hz. They correspond to the following five pairs **e**−**q**, **i**−**m**, **g**−**p**, **a**−**m**, and **e**−**f**, and they concern only the eight peaks **a**, **e**, **f**, **g**, **i**, **m**, **p**, and **q**, as **e** and **m** appear 2 times. As shown above, **e** belongs to PW_8, and **m**, to PW_9,

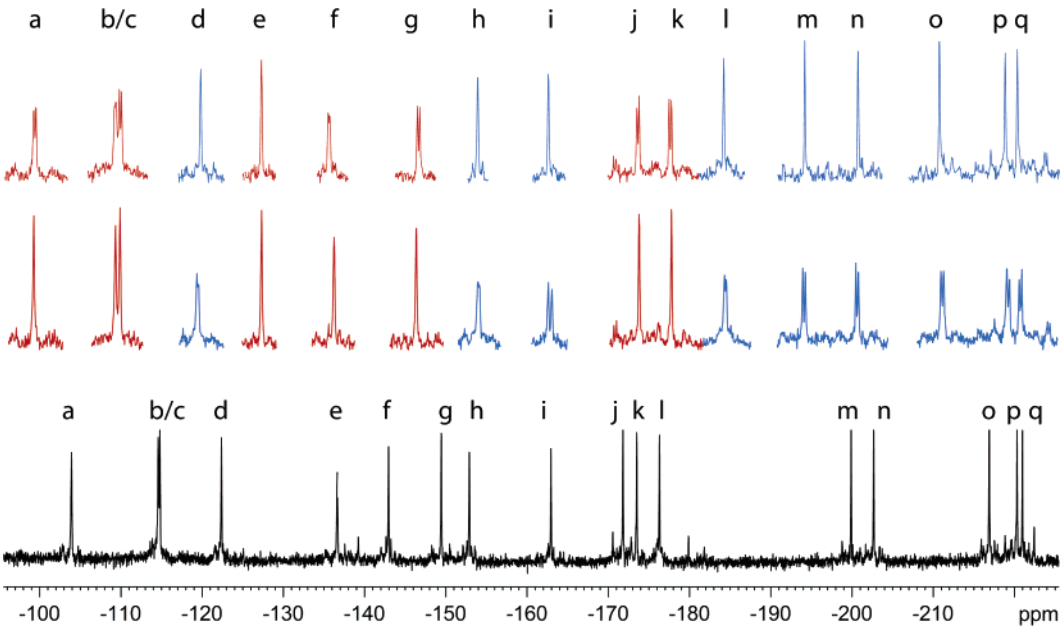

Figure 3. 12.5 MHz ^{183}W NMR spectra of α_1-$[P_2W_{17}O_{61}]^{10-}$ (2 g/mL) with broad-band ^{31}P decoupling (bottom trace) and with selective $^2J_{W-P}$ decoupling from the phosphorus in the PW_8 unit (middle trace) and in the PW_9 unit (top trace). Signals belonging to the PW_8 unit are in red, and those of the PW_9 unit, in blue.

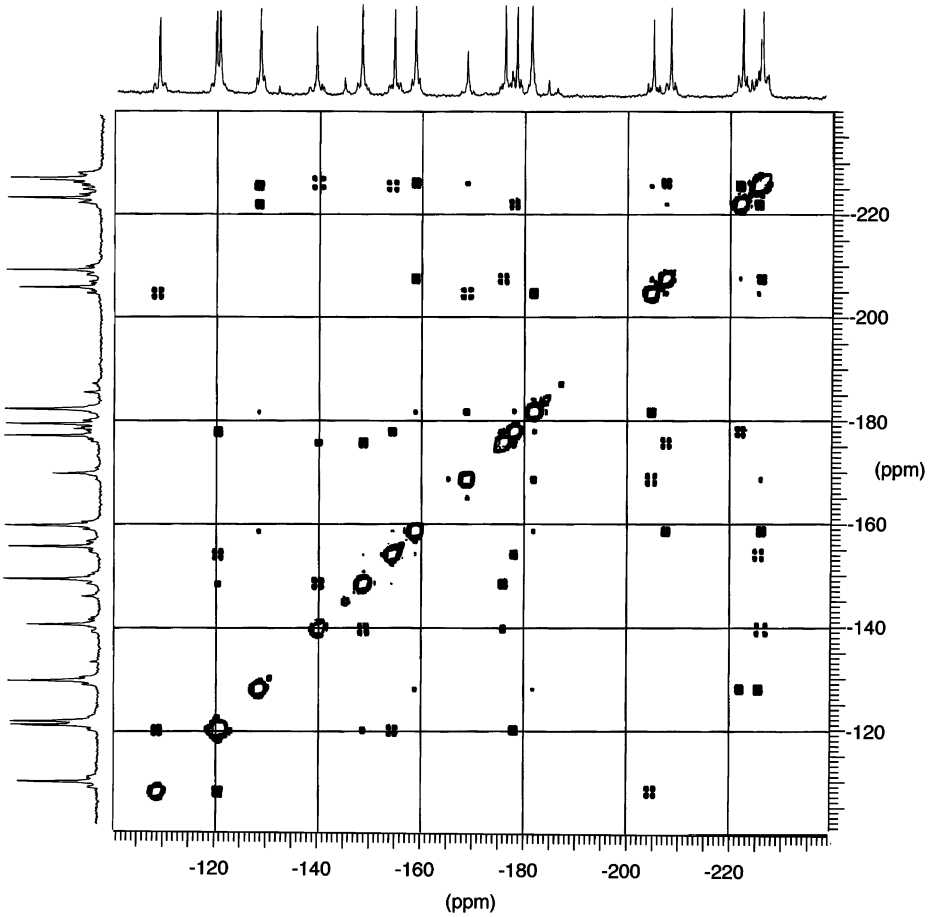

Figure 4. 2D COSY ^{183}W NMR spectrum of α_1-$[P_2W_{17}O_{61}]^{10-}$ (ca. 3 g/mL, 283 K, 20.8 MHz, total spectrometer time 71 h).

respectively, and as only W5, W9 (both in PW_8), and W15 (in PW_9) are expected to have two very large coupling constants, **m** must be assigned to W15 (Figure 1). This becomes our starting point. Because of the "cyclic" nature of the POM framework, further assignment can follow different pathways and can be cross-checked at nearly each step. Among the neighbors of W15, only W9 belongs to PW_8, and consequently **a** ≡ W9. The **m**−**i** correlation corresponds to the intra-PW_9 W10−W15 coupling (strong type B), and consequently **i** ≡ W10. The last significant correlation of **m**, **m**−**l**, corresponds

Table 3. 2D-COSY Data for α_1-$[P_2W_{17}O_{61}]^{10-}$ (from Figure 4)[a,b]

peak W	a 9	b/c 1 + 3	**d** 18	e 5	f 2	g 8	**h** 17	**i** 10	j 6	k 7	**l** 16	**m** 15	**n** 12	**o** 13	**p** 14	**q** 11
a 9	**−108.4**	21.1 A/S				e/vw						27.4 C/S				
b/c 1+3	21.9 A/S	**−120.3**			<10 e/w	24.3 A				16.4 A						
d 18			**−128.3**				<10 e				<10 e			16.4 A	19.6 A	
e 5				**−140.0**	27.4 A/S				<10 B/w							36 C/S
f 2		<10 e/w		27.4 A/S	**−148.8**				18 A							
g 8	e/vw	25.0 A				**−154.2**	*			14.9 B					28.2 C	
h 17			<10 e			*	**−159.0**				<10 e		16.4 A			19.6 A
i 10								**−168.6**			<10 A/w	29.7 B/S				<10 e/S
j 6				10 B/w	18.8 A				**−175.8**	* e/w			25.8 C			
k 7		15.7 A				14.9 B			* e/w	**−177.9**	*			23.5 C		
l 16			<10 e				<10 e	<10 A/w		*	**−181.7**	17.2 A				
m 15	28.2 C/S							29 B/S			15.7 A	**−204.7**	*		<10 e/w	
n 12							17.2 A		25.8 C			*	**−207.5**	<10 e		20.3 B
o 13			16.4 A							24.3 C			<10 e	**−222.0**	19.6 B	
p 14			19.6 A			29 C						<10 e/w		20.3 B	**−225.6**	
q 11				35.2 C/S			20.3 A	<10 e/S					20.3 B			**−226.2**

[a] * represents questionable cross-peak near the diagonal. [b] Peak lettering corresponds to the order of signals in the ^{183}W spectrum (see Figure 2). Underlined letters correspond to peaks of the PW_9 unit as shown by selective $^2J_{W-P}$ decoupling. Tungsten numbering corresponds to the final assignment. On diagonal: δ in ppm. Off diagonal: J in Hz determined by row analysis and type of coupling. The empirical order of coupling constants is e (edge) < A (cap−belt corner) ≈ B (intraunit belt−belt corner) < C (interunit belt−belt corner). Expected modifications due to the lacuna are noted: vw = very weaker, w = weaker, S = stronger than usual.

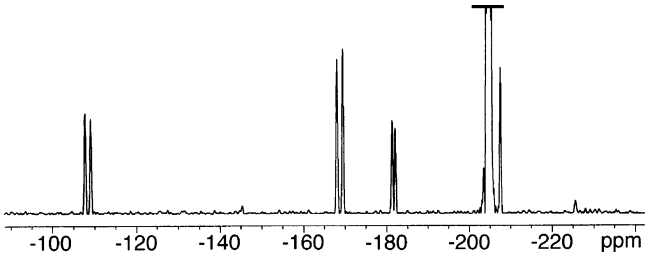

Figure 5. Row analysis of peak **m** (−204.7 ppm) in the 2D COSY spectrum of α_1-$[P_2W_{17}O_{61}]^{10-}$ to measure the $^2J_{W-W}$ coupling constants.

to the cap−belt W15−W16 coupling (type A), and consequently **l** ≡ W16.

The second peak with two strong couplings **e** necessarily corresponds to W5, then **q** ≡ W11 and **f** ≡ W2, because they belong to PW_9 and PW_8, respectively. This agrees with the **i**−**q** ≡ W10−W11 correlation. One should notice that the **e**−**q** ≡ W5−W11 coupling constant is the largest $^2J_{W-W}$ value observed, as expected for this interunit (type C) coupling involving a W bordering the lacuna. To finish with **e** ≡ W5, its correlation with **j** has to be assigned to the W5−W6 corner coupling, smaller than usual because of the direct trans influence, and consequently **j** ≡ W6. Again, this agrees with the **j**−**f** correlation for a normal cap−belt W2−W6 type A coupling. The third corner coupling of **j** indicates that **n** ≡ W12. Furthermore, the **q**−**h** correlation leads to assigning **h** ≡ W17. This is corroborated by the **q**−**n** ≡ W11−W12 corner coupling.

Among the remaining peaks of PW_8 (**b**/**c**, **g**, **k**), **g** and **k** must be in the belt (W7, W8) because they have type C couplings to the PW_9 unit. Therefore, the overlapping signals **b** and **c** correspond to W1 and W3. Similarly for PW_9, **o** and **p** (both with three strong couplings) are assigned to the belt atoms W13, W14 of PW_9 and **d** is assigned to the cap atom W18. The **m**−**p** (small) and **p**−**g** (strong) correlations lead to assigning **p** to W14 and then **g** to W8. This leaves **k** ≡ W7 and **o** ≡ W13 to complete the unambiguous assignment of α_1-P_2W_{17}.

C. Comments on the ^{183}W Chemical Shifts of α_1-P_2W_{17}. The chemical shifts can be compared to those of the parent saturated anion α-$[P_2W_{18}O_{62}]^{6-}$ (δ_{cap} = −126.5, δ_{belt} = −172 ppm).[23,29]

For the PW_9 unit, all belt nuclei are strongly shielded (−30 to −50 ppm) except W10, near the lacuna. Although more remote from the lacuna, the chemical shift differences of the cap nuclei are quite large with W16 being strongly shielded, whereas W18 is nearly at the same δ as that for P_2W_{18}.

(29) ^{183}W chemical shifts of polyoxotungstates are very sensitive to medium effects, such as concentration, solvent, ionic strength, and pH; therefore relatively small variations (of ca. 5 ppm) between the lacunary and the saturated POM are hardly interpreted as due to authentic chemical shift variations.

For the PW_8 unit, the two remote belt nuclei W6 and W7, as well as the two cap nuclei W1 and W3, are globally unaffected. The other belt nuclei are deshielded, especially those near the lacuna W5 (+ 30 ppm) and W9 (+60 ppm, corner junction to the lacuna). Surprisingly, the cap nucleus W2 is shielded by ca. 20 ppm.

To summarize the results for the four atoms near the lacuna, W1 and W10 (both "corner" linked) are nearly unaffected, and W5 ("corner" linked) and particulary W9 ("edge" linked) both in the defect belt are significantly deshielded.

From these observations, as also from recent DFT calculations,[8] it seems extremely difficult to rationalize the ^{183}W chemical shifts by taking into account both the global increase of the anionic charge and the overall charge redistribution induced by removal of $\{WO\}^{4+}$.

D. Comments on the $^2J_{W-W}$ Coupling Constants. Coupling is uncertain for the W6−W7 pair, with too close peaks **j** and **k**, and of course not detectable for the W1−W3 pair (same chemical shift **b** and **c**). No cross-peak is observed for the correlation between W8 and W9 (**a** and **g**). This is consistent with a very low edge coupling because of the trans influence at the lacuna. All other two-bond W−O−W interactions give rise to cross-peaks.

The assignment of the type of different edge and corner couplings has been added to Table 3. As can be seen, most $^2J_{w-w}$ values fall into the expected range and are consistent with other polyoxotungstates. However, some coupling constants involving W7 and W8 deviate slightly, indicating that the lacuna induces small structural changes even at remote sites.[13]

E. Comments on the Relaxation Times T_1. The longitudinal relaxation time T_1 of ^{183}W nuclei is dominated by a chemical shift anisotropy mechanism expressed in eq 1.

$$\frac{1}{T_1^{(CSA)}} = \frac{2}{15}\gamma^2 B_0{}^2 \Delta\sigma^2 \tau_c \qquad (1)$$

where γ = gyromagnetic ratio, B_0 = magnetic field, τ_c = rotational correlation time, and $\Delta\sigma = \sigma_{||} - \sigma_{\perp}$ represents the chemical shift anisotropy (CSA) of the observed nucleus.

Longitudinal relaxation rates for the 17 peaks of α_1-P_2W_{17} have been measured at 12.5 MHz (AC300, 7 T) and 20.8 MHz (DRX500, 12 T) and are compiled in Table 4. In agreement with the above formula the relaxation times determined at 7 T are ca. 3 times higher than those measured at 12 T. Moreover, there is a significant dispersion of the T_1 values for the different ^{183}W resonances. The most slowly relaxing nuclei are (in the order of increasing relaxation rate) W10 < W1/3 ≈ W5 ≈ W15. They all are nuclei which share atypical coupling contants. The usual geometry of a $\{WO_6\}$ in saturated POMs, that is a distorted octahedron with nearly C_{4v} symmetry, results in a relatively large CSA, which was directly accessible only in the case of the highly symmetrical $[PW_{12}O_{40}]^{3-}$ by ^{183}W MAS solid-state NMR.[30] As shown in eq 1, the relaxation times also allow the determination of the CSA, if the correlation times τ_c are known. We believe that the rigid structure of the oxo-cluster α_1-P_2W_{17} with its solvent shell leads to quasi-isotropic tumbling in solution and, therefore, to similar τ_c for all W. Then, comparison of T_1 allows the evaluation of the relative values of CSA. Hence surprisingly, the slow relaxation indicates a reduced CSA of the nuclei with atypical environments and, thus, demonstrates that the presence of the lacuna renders the coordination sphere of the nearby W atoms more symmetrical.

(30) Knight, C. T. G.; Turner, G. L.; Kirkpatrick, R. J.; Oldfield, E. *J. Am. Chem. Soc.* **1986**, *108*, 7426−7427.

Table 4. Longitudinal Relaxation Times T_1 for All Tungsten Atoms in α_1-$[P_2W_{17}O_{61}]^{10-}$ Measured at 300 K at Two Different Magnetic Fields; Accuracy ± 20%

W	$-\delta^a$ (ppm)	T_1 (ms) (20.8 MHz)	T_1 (ms) (12.5 MHz)
1/3	120.3	250	700
2	148.4	200	600
1/3	120.5	350	1000
5	139.8	350	1000
6	175.8	350	900
7	177.9	300	800
8	154.2	300	800
9	108.5	300	900
10	168.7	700	2000
11	226.1	300	800
12	207.5	300	900
13	222.0	300	800
14	225.5	250	700
15	204.7	350	1000
16	181.7	250	700
17	158.7	200	600
18	128.2	200	600

[a] The differences in δ compared to Table 3 result from the different temperatures.

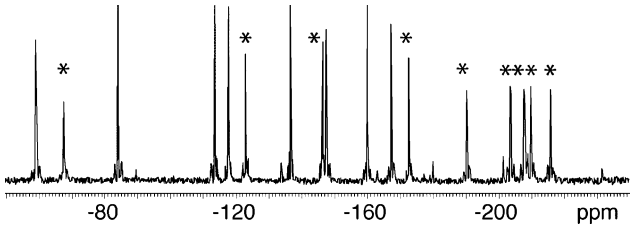

Figure 6. ^{31}P coupled ^{183}W NMR spectrum of α_1-$[YbP_2W_{17}O_{61}]^{7-}$ (ca. 1 g/mL). $^2J_{W-P}$ coupling is apparent for signals belonging to the PW_9 subunit, which appear as doublets (smaller peaks marked with an asterisk).

NMR Spectra of α_1-$[YbP_2W_{17}O_{61}]^{7-}$. In solution, the complex α_1-$[Ce^{III}P_2W_{17}O_{61}]^{7-}$ was shown to be in fast equilibrium with its dimer $[\{\alpha_1\text{-}Ce^{III}P_2W_{17}O_{61}\}_2]^{14-}$.[10] A similar monomer−dimer equilibrium might exist for α_1-YbP_2W_{17}, but this has no influence on the following strategy of peak assignment.

A. Partial Assignment to Each PW_9 or PW_8Yb Subunit of α_1-YbP_2W_{17}. Observation of the $^2J_{W-P}$ coupling requires high resolution ^{183}W spectra obtained with relatively low concentrated solutions. The spectrum of Figure 6 was run with ca. 1 g/mL of α_1-YbP_2W_{17} in aqueous solution. We found by additional analysis that some chemical shifts depend highly on the POM concentration leading to the crossover of two signals around −120 ppm. In the following, the denomination of the lines in alphabetic order corresponds to the relative positions observed in the very concentrated solution used for the 2D COSY analysis.

Among the 17 resonances of the ^{183}W spectrum of α_1-YbP_2W_{17}, only nine lines appear as doublets under high-resolution conditions, that is **b**, **e**, **h**, **l**, **m**, **n**, **o**, **p** and **q** (Figure 6). All these doublets coalesce to singlets by selective ^{31}P decoupling at the frequency of the PW_9 subunit. Accordingly, these resonances are assigned to W atoms belonging to the PW_9 subunit. The remaining eight resonances **a**, **c**, **d**, **f**, **g**, **i**, **j**, **k** are then assigned to the PW_8Yb subunit. One might be tempted to

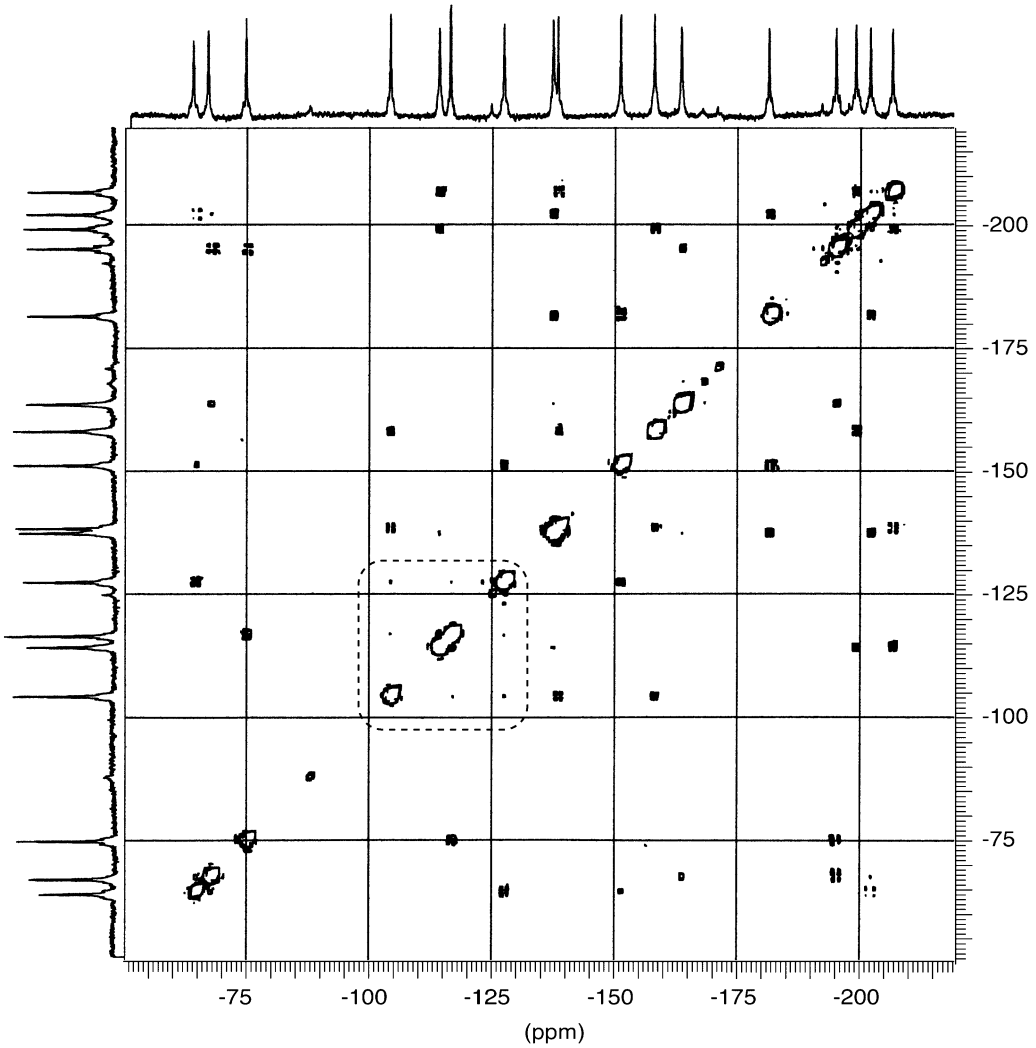

Figure 7. 2D COSY ^{183}W NMR spectrum of α_1-$[YbP_2W_{17}O_{61}]^{7-}$ (ca. 3 g/mL, 300 K, 20.8 MHz, total spectrometer time 75 h). Inside the dotted frame are three signals (**d**, **f**, **g**) with mutual cross-peaks used to start the asignment.

assign **e**, **h** and **l** to cap nuclei, because of their significantly smaller $^2J_{W-P}$ coupling constants (Table 2). However, the influence of the lacuna on the $^2J_{W-P}$ coupling (by deformation of the structure) cannot be predicted, and therefore this assignment should not be taken for granted. The following will prove that it is nevertheless correct.

B. Analysis of the 2D-COSY Spectrum of α_1-YbP_2W_{17}. Because α_1-YbP_2W_{17} does not isomerize quickly to α_2, its 2D-COSY spectrum could be registered at 300 K, which leads to less broad signals than those at lower temperature (Figure 7).

A first inspection of the contour plot COSY spectrum (Figure 7) allows us to recognize three diagonal peaks, namely **d**, **f**, and **g** of the PW_8Yb subunit, with mutual low intensity cross-peaks. They must be assigned to cap nuclei, that is W1, W2, and W3. As **f** shares only one strong coupling (with **c**), it might be assigned to W1 and **c** assigned to W9. The second strong coupling of **c** (with **n**) leads to **n** ≡ W15. One might verify that **n** corrresponds to a W in the PW_9 unit according to the selective decoupling experiments. This type of cross-check will not be commented on in the following but can be retrieved from the experimental correlation matrix (Table 5). From the strong couplings of **n** with both **l** and **b**, these two signals, which share a medium-intensity cross-peak, must be assigned to (W10, W16). The low-intensity cross-peak between **b** and **p**, which has three strong couplings, is consistent with **p** ≡ W11 and **b** ≡ W10 and, therefore, **l** ≡ W16. Both **l** and **p** are coupled to **h**; therefore **h** ≡ W17. **h** presents another strong coupling to **m** and another weak coupling to **e**, leading to **m** ≡ W12 and **e** ≡ W18. Note that **e**, **l**, and **h** are ^{183}W resonances with very small $^2J_{W-P}$ couplings (≤ 1 Hz), as expected for cap nuclei in a saturated Dawson subunit (see above).

The two peaks **o** and **q** which correlate to **e** (≡ W18) correspond to the remaining belt atoms of PW_9 (W13, W14). To answer this indetermination, we have to search for a cross-peak between **o** (or **q**) and **n** (≡ W15) or **m** (≡ W12). We failed to identify any such peak, likely because the experimental conditions for the 2D spectrum were not optimized for such very low couplings. Similarly, for the same reason (lack of observable small-coupling correlations) the PW_8Yb-"vis-à-vis" (W7, W8) of W13 and W14 could not be discriminated. Instead of repeating the 2D-COSY experiment with a larger initial delay (so-called long-range 2D-COSY experiment), we preferred to register its 1D alternative using a selective excitation (by a Gaussian-shaped pulse) of **m**, allowing the magnetization to flow from W12 only. The delay between the two pulses was chosen to give a maximal response for $^2J_{W-W}$ ca. 10 Hz. The obtained spectrum (Figure S1, Supporting Information) shows clearly a

Table 5. 2D-COSY Data for α_1-$[YbP_2W_{17}O_{61}]^{7-}$ (from Figure 7)[a–c]

peak W	a 5	**b** 10	c 9	d 3	**e*** 18	f 1	**g** 2	**h** 17	i 8	j 6	k 7	**l** 16	**m** 12	**n** 15	**o** 13	**p** 11	**q** 14
a 5	–64.6						23.3 A/S			<10 B/w						35.3 C/S	
b 10		–67.7										8.6 A/w		27.6 B/S		<10 e/S	
c 9			–75.0			22.4 A/S			e/w					30.2 C/S			
d 3				–104.3		<10 e/vw	<10 e/w		22.4 A		19.8 A						
e* 18					–114.3			<10 e				e			17.2 A		20.7 A
f 1			20.7 A/S	<10 e/vw		–116.7	<10 e/w										
g 2	25.0 A/S			<10 e/w		<10 e/w	–127.5			20.7 A/S							
h 17					<10 e			–137.5				e	19 A			19 A	
i 8			e/w	23.3 A					–138.5		14.7 B						28.4 C
j 6	<10 B/w						17.2 A			–151.3	e		25.9 C				
k 7				16.4 A					14.7 B	e	–158.2				25 C		
l 16		9.5 A/w			e			<10 e				–163.7		15.5 A			
m 12								15.5 A		27.6 C			–181.6		5.6*** e	20.7 B	
n 15		26.7 B/S	29.3 C/S									15.5 A		–195.2			e/w
o 13					14.7 A						25 C		5.6*** e		–199.2		20.7 B
p 11	33.6 C/S	<10 e						19.0 A					21.6 B		**	–202.3	**
q 14					19.8 A				29.3 C					e/w	19.0 B		–206.7

[a] δ in ppm on the diagonal; J in Hz at the intersection of rows and columns. Underlined letters correspond to peaks of the PW_9 unit as shown by selective $^2J_{W-P}$ decoupling. [b] * The order of signals e and f changes depending on the concentration. ** represents undefined cross-peak near the diagonal. *** Obtained from 1D-COSY (Supporting Information). [c] The empirical order of coupling constants is e (edge) < A (cap−belt corner) < B (intraunit belt−belt corner) < C (interunit belt−belt corner). Expected modifications due to the lacuna are noted: vw = very weaker, w = weaker, S = stronger than usual.

correlation with peak **o** (5.6 Hz). This result demonstrates unambiguously that **o** ≡ W13 and consequently **q** ≡ W14.

The belt nuclei in the PW_8Yb unit could then be easily assigned starting from their belt partners of the PW_9 unit, that is, **i** ≡ W8 (strong correlation with **q** ≡ W14), **k** ≡ W7 (correlation with **o** ≡ W13), **j** ≡ W6 (correlation with **m** ≡ W12), and **a** ≡ W5 (correlation with **p** ≡ W11). Finally, **d** and **g** are assigned to W3 and W2, respectively, thanks to the cross-peaks with **i** ≡ W8 and **k** ≡ W7 and with **a** ≡ W5 and **j** ≡ W6.

C. Comments on the ^{183}W Chemical Shifts of α_1-YbP_2W_{17} as Compared with α_1-P_2W_{17}. Surprisingly, and contrary to the ^{31}P NMR data, the ^{183}W NMR spectrum of α_1-$P_2W_{17}Yb$ is not strongly affected by the coordination of the lanthanide cation Yb^{3+}. In particular, the changes of δ are relatively moderate and all resonances are relatively narrow, as is the case for a diamagnetic compound. This is in contrast to the ^{183}W spectra of other lanthanide POM derivatives: for example, in the Ce^{III} complexes of α_2-P_2W_{17}, the resonances of the W nuclei μ-oxo bonded to the cerium atom are broad and strongly deshielded.[31]

The presence of Yb^{3+} induces less dramatic effects on the nearby nuclei: hence W9 is deshielded by only ca. 20 ppm,

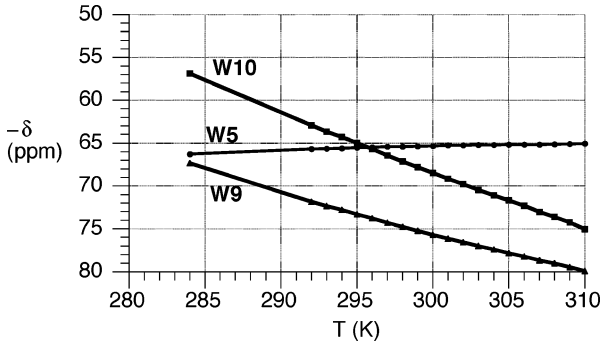

Figure 8. Chemical shift variation as a function of temperature of selected peaks bordering the lacuna in the ^{183}W NMR spectrum of α_1-YbP_2W_{17}.

and W1 is surprisingly almost invariant with respect to α_1-P_2W_{17}. Only W5 and W10 are deshielded by nearly 100 ppm.

Further influence of the paramagnetic center is better revealed by the strong negative temperature coefficient for both W9 and W10 (0.446 ppm K^{-1} and 0.666 ppm K^{-1}, respectively, Figure 8), whereas all other nuclei experience positive and relatively small coefficients (less than 0.16 ppm K^{-1}, Figure S2, Supporting Information).

D. Comments on the $^2J_{W-W}$ Coupling Constants. Comparison of the corresponding coupling constants in α_1-P_2W_{17}

(31) Racimor, D., Ph.D. Thesis, Université Pierre et Marie Curie, 2003.

Table 6. Mean Values of the $^2J_{W-W}$ Corner Coupling Constants (Hz)

junction	α_1-$[P_2W_{17}O_{61}]^{10-}$	α_1-$[YbP_2W_{17}O_{61}]^{7-}$
A: cap−belt in PW_8/$YbPW_8$	21.6	21.1
A: cap−belt in PW_9	16.6	16.1
B: belt−belt	18.9	18.6
C: belt−belt	28.4	29.0

and α_1-YbP_2W_{17} (Tables 3, 5, and 6) reveals immediately that Yb^{3+} does not induce strong modifications. In particular, contrary to what is observed for diamagnetic POM complexes of transition metals, the "atypical" coupling constants present in the lacunary POM α_1-P_2W_{17} are not restored to "normal" values in the complex α_1-YbP_2W_{17}. This can be interpreted by a relatively small variation of the geometrical arrangement of the atoms around the lacuna on complex formation. The larger Yb^{3+} ion is sitting outside the lacuna.

Conclusions

We have shown here that it is possible to assign completely the peaks of a ^{183}W spectrum even in the absence of an easily recognized signal. Our strategy is based on the interpretation of the $^2J_{W-W}$ coupling constants, together with the $^2J_{W-P}$ coupling. The results indicate that the presence of the lacuna influences the chemical shifts of the surrounding W atoms, but no simple correlation can be established to rationalize the chemical shifts. They should be used in a more complete analysis of the charge distribution over the whole structure. The data obtained on α_1-YbP_2W_{17} show that the complexation of the lanthanide does not significantly modify the POM framework, not even the geometry of the lacuna.

For us, these results represent the starting point for the study of diastereomers formed by α_1-YbP_2W_{17} and chiral ligands. We are investigating the sites where the chiral molecules interact, and these results will be presented in a subsequent publication.

Experimental Section

$K_9Li\alpha_1$-$[P_2W_{17}O_{61}]$[32] and $K_7\alpha_1$-$[YbP_2W_{17}O_{61}]$[18] were prepared according to literature methods and checked by IR and ^{31}P NMR spectroscopy.

^{183}W NMR spectra were recorded in 10 mm o.d. tubes at 12.5 MHz on a Bruker AC300 spectrometer equipped with a low-frequency special VSP probehead and at 20.8 MHz on a Bruker AM500 spectrometer with a standard tunable BBO probehead. The highest resolution, for the determination of $^2J_{W-P}$ coupling constants, was obtained at the lower field (AC300), whereas the higher field (DRX500) gave the highest sensitivity spectra for determination of $^2J_{W-W}$ coupling constants. Chemical shifts are referenced to WO_4^{2-} ($\delta = 0$ ppm) according to the IUPAC recommendation: positive δ corresponds to high-frequency shift (deshielding) with respect to the reference. They were measured by the substitution method, using a saturated aqueous solution (in D_2O) of dodecatungstosilicic acid ($H_4SiW_{12}O_{40}$) as a secondary standard ($\delta = -103.8$ ppm). The spectral width for the 1D spectra was ca. 200 ppm (ca. 2500 Hz). High quality spectra, with good signal-to-noise ratio to observe tungsten satellites, required at least 10^5 transients corresponding to more than 2 days of spectrometer time.

^{31}P spectra were recorded in 5 mm o.d. tubes at 121.5 MHz on a Bruker AC300 spectrometer equipped with a QNP probehead. Chemical shifts are referenced to 85% H_3PO_4. ^{31}P spectra were also measured prior to ^{183}W spectra on the same NMR tubes on the decoupling coil of the VSP probehead, both for control and for determination of the ^{31}P decoupling frequency. The ^{31}P decoupling experiments were performed with a B-SV3 unit operating at 121.5 MHz and equipped with a B-BM1 broad band modulator. Selective or broad-band decoupling was determined by appropriate choice of the synthesizer frequency and of the output power (5−40 W) before entering the decoupling coil of the low-frequency probehead. The $^{31}P-^{183}W$ INEPT polarization transfer experiment was performed using the low-frequency VSP probehead on a Bruker Avance 300 spectrometer equipped with a third observation channel: because of the very low values of the $^2J_{W-P}$ coupling constants, long interpulse delays, in the order of 500 ms, were required for an efficient transfer.

The highly concentrated solutions for the 2D spectra were prepared by dissolving the potassium salt (6.8 g for both α_1-P_2W_{17} and α_1-YbP_2W_{17}) in 2.5 mL of saturated $LiClO_4$ aqueous solution. After filtering off the precipitate ($KClO_4$), the filtrate was added with 0.3 mL of D_2O for field frequency lock. The ^{183}W 2D-COSY spectra were obtained at 20.8 MHz on the DRX500 Bruker spectrometer, using a simple Jeener (90°-incremental delay−90°-acquisition−relaxation delay) pulse sequence. The spectral widths were 3200 Hz (154 ppm) and 3500 Hz (168 ppm) for α_1-P_2W_{17} and α_1-YbP_2W_{17} respectively. In each case 4200 transients were acquired with the sum of acquistion time and relaxation delay reaching 500 ms. The number of stored experiments (t_1 dimension) were 114 for α_1-P_2W_{17} and 128 for α_1-YbP_2W_{17} with a total spectrometer time of 71 and 75 h, respectively. The data were zero-filled and apodized with a sine bell function before Fourier transformation. The resulting COSY maps (Figures 4 and 7) are presented as a power spectrum after symmetrisation of the transformed matrix.

Longitudinal relaxation times (T_1) were measured on nondeaerated solutions, using the classical IRFT (inversion−recovery Fourier transform) pulse sequence. The T_1 values were determined from the zero of the expression $I(t)$, according to $I(t) = I(\infty) \times [1 - 2 \times \exp(t/T_1)]$ where t represents the delay between the successive pulses: $T_1 = t_{(I=0)}/0.69$; in the present case, this zero method gives more reliable T_1 values than those afforded by curve fit analysis of $I(t)$ vs t because of the relatively poor signal-to-noise ratio of the spectra as well as the difficulty in obtaining the flat baselines required by the automatic curve fit program. The accuracy for the T_1 values was evaluated to be ca. 20%.

Acknowledgment. NMR measurements (DRX500) were performed at the NMR facility center (SIARE) of the University Pierre and Marie Curie. We are grateful to our university and the CNRS for financial support.

Note added in proof: After submission of the manuscript, two important papers on density-functional calculations of the ^{183}W and ^{17}O NMR chemical shifts for large polyoxometalates were published.[33,34] Although these calculations reproduce the patterns of the chemical shifts for several types of tungsten atoms, the accuracy of the calculations is not sufficient to assign individual signals of a polyoxotungstate, in particular when the range of chemical shifts is rather narrow.

Supporting Information Available: Tables of $^2J_{W-W}$ coupling constants in α_1-P_2W_{17} and α_1-YbP_2W_{17}. 1D-COSY spectrum of α_1-YbP_2W_{17} (selective excitation of peak **m**). Charts displaying the chemical shifts of all tungsten atoms in α_1-$[YbP_2W_{17}O_{61}]^{7-}$ as a function of temperature. This material is available free of charge via the Internet at http://pubs.acs.org.

JA0575934

(32) Contant, R. *Inorg. Synth.* **1990**, *27*, 104−111.

(33) Gracia, J.; Poblet, J. M.; Autschbach, J.; Kazansky, L. P. *Eur. J. Inorg. Chem.* **2006**, 1139−1148.

(34) Gracia, J.; Poblet, J. M.; Fernandez, J. A.; Autschbach, J.; Kazansky, L. P. *Eur. J. Inorg. Chem.* **2006**, 1149−1154.